ISSN 1606-867X (Print)
ISSN 2687-0711 (Online)
Condensed Matter and Interphases
Kondensirovannye Sredy i Mezhfaznye Granitsy
https://journals.vsu.ru/kcmf/

Original articles

Research article
https://doi.org/10.17308/kcmf.2024.26/12229

Nanocrystalline films based on $YCrO_3$ and $LaCrO_3$ yttrium and lanthanum chromites doped with strontium ions Sr^{2+} as a basis for semiconductor gas sensors

M. A. Yakimchuk✉, E. S. Eliseeva, V. F. Kostryukov

Voronezh State University,
Universitetskaya pl. 1, Voronezh 394018, Russian Federation

Abstract

For the production of gas-sensitive sensors, easily obtained nanostructured substances are required. Therefore, one of the most important scientific problems is the search for new compositions and an improvement in the used materials. The aim of this study was the creation of thin-film materials based on yttrium and lanthanum chromite nanopowders$YCrO_3$ and $LaCrO_3$, doped with strontium ions, and the identification of their gas-sensitive properties.

The synthesis of nanopowders was carried out by the sol-gel method for $LaCrO_3$ and the citrate method for $YCrO_3$. Doped powders were obtained using the same synthesis methods as the original samples. The phase and elemental composition of the obtained samples was determined. The result of this study demonstrated that the actual composition of the nanopowders is close to the nominal one. Gas-sensitive properties were determined by measuring the specific surface resistance of the obtained samples to the content of carbon monoxide CO with a concentration of 50 ppm.

It was found that the obtained samples possess *n*-type of conductivity and a good response to the presence of traces of carbon monoxide. Yttrium chromite-based nanofilms exhibit better gas-sensitive response compared to $LaCrO_3$. The maximum value was obtained for $Y_{0.9}Sr_{0.1}CrO_3$, demonstrating a gas sensitive response of 2.83 at a temperature of 200 °C.

Keywords: Semiconductors, Gas sensitivity, Yttrium chromite, Lanthanum chromite, Doping, Nanofilms, Nanopowders

Acknowledgements: The results of the research were obtained using the equipment of the Centre for the Collective Use of Scientific Equipment of Voronezh State University.

For citation: Yakimchuk M. A., Eliseeva E. S., Kostryukov V. F. Nanocrystalline films based on $YCrO_3$ and $LaCrO_3$ yttrium and lanthanum chromites doped with strontium ions Sr^{2+} as a basis for semiconductor gas sensors. *Condensed Matter and Interphases*. 2024;26(3): 536–546. https://doi.org/10.17308/kcmf.2024.26/12229

Для цитирования: Якимчук М. А., Елисеева Е. С., Кострюков В. Ф. Нанокристаллические пленки на основе хромитов иттрия и лантана $YCrO_3$ и $LaCrO_3$, допированных ионами стронция Sr^{2+} как основа полупроводниковых газовых сенсоров. *Конденсированные среды и межфазные границы*. 2024;26(3): 536–546. https://doi.org/10.17308/kcmf.2024.26/12229

✉ Milena A. Yakimchuk, e-mail: yakimchuk.720.46@gmail.com

1. Introduction

Production safety is one of the main problems today. Emitted toxic gases require immediate detection for subsequent timely elimination. Therefore, gas-sensitive sensors are used; and the search for modern material compositions that allow detecting small concentrations of gases in a short time is carried out.

Today, gas sensors based on *n*-type semiconductors are widely used. The most significant progress was achieved in the development of gas-sensing transistors, Schottky barrier devices, and semiconductor gas-sensing resistors [1]. All semiconductors with the electronic type of conductivity have a sensory response, but wide-bandgap semiconductors are widely used. Such semiconductors include: SnO_2, ZnO, In_2O_3, WO_3, characterized by the highest gas sensitivity. Important physical and chemical properties of these materials are the electronic type of conductivity, transparency in a wide range of the electromagnetic radiation spectrum and high surface reactivity [2–6]. At the same time, semiconductors with p-type conductivity can also act as gas sensors [7], however, in this case, oxidizing gases act as priority detected gases.

The need for detector selectivity leads to the search for more complex structural compounds, one of which is the perovskite – orthorhombic structure of the Pbmn spatial group with the general formula ABO3. There is a wide variety of gas sensors with a perovskite structure capable of detecting various gases and volatile compounds.

One of common material is a composite of iron oxide and lanthanum oxide, of perovskite type $LaFeO_3$. It has both high ionic and electronic conductivity at high temperatures and is suitable for detecting gases such as butane, propane, propylene, butylenes, ethylene, methane, formaldehyde, and carbon dioxide [8–10].

In addition to lanthanum ferrite, its close analogue, lanthanum cobaltite, is also actively used, which exhibits satisfactory sensory properties for reducing gases such as carbon monoxide and ammonia vapors [11].

Alternative gas sensors with a perovskite structure are transition metal chromites. Their main advantage is the ability to detect inorganic gases – carbon monoxide and dioxide, nitrogen oxide (II) [12, 13]. Gas detection occurs at slightly higher concentrations of gases than when using a lanthanum ferrite-based gas sensor. The response time and recovery time is up to 3 minutes, however, with a higher concentration of the test gas. Chromites are also promising due to their low cost, selectivity for specific gases and mechanical strength, although the operating temperatures of the sensors also remain high [14-16]. Due to its simplicity and cost-effectiveness, the sol-gel method remains the main method of synthesis of such materials [17-19].

Further developments in chromite-based gas sensors are aimed at reducing operating temperatures and gas concentrations required for detection. The aim of this study was to create nanocrystalline films based on yttrium and lanthanum chromite nanopowders doped with strontium ions, as well as to identify their gas-sensitive properties depending on the dopant content.

2. Experimental

Doped nanopowders of lanthanum chromite were obtained by the sol-gel method. The work used a technique used in our laboratory for the synthesis of ferrites [20], and adapted for lanthanum chromite. A mixture of $La(NO_3)_3$, $Cr(NO_3)_3$, and $Sr(NO_3)_2$ solutions was added to boiling water with constant stirring using a magnetic stirrer, based on their stoichiometric ratios to obtain $LaCrO_3$, $La_{0.95}Sr_{0.05}CrO_3$, and $La_{0.9}Sr_{0.1}CrO_3$. The resulting solutions were boiled for 5 min. Then, while stirring, ammonia water was added dropwise through a separatory funnel, taken in a quantity sufficient for the complete precipitation of cations, based on the stoichiometric ratio of the reagents. The solutions were stirred for another 5 min. The resulting precipitates were separated on a vacuum filter and dried for several days to constant weight at room temperature. The final nanopowders were obtained by heat treatment of dehydrated precipitates in a muffle furnace (SNOL 8.2/1100) at a temperature of 950 °C for 1 h.

The citrate method was used to obtain yttrium chromite (with and without dopant). The technique was also similar to that of the synthesis of yttrium ferrite [21] and adapted for chromite. The $Cr(NO_3)_3 \cdot 9H_2O$, $Y(NO_3)_3 \cdot 6H_2O$, and $Sr(NO_3)_3 \cdot 4H_2O$ were dissolved in distilled water

in stoichiometric proportion. The solutions were heated for better dissolution of the salts and then cooled. Then, while stirring, the calculated amount of ammonia was added dropwise until precipitate was formed. After the addition of citric acid, it was heated again until the precipitate dissolved. The solutions were then completely evaporated and burned until ash was formed. The resulting powders were annealed in a muffle furnace (SNOL 8.2/1100) at a temperature of 950 °C for 1 h.

For the study of the gas-sensitive properties, the synthesized powders were dispersed in ethyl alcohol with the addition of cetyltrimethylammonium bromide (CTAB) as a surfactant until a paste was formed. Then the synthesized powders were applied to a conductive element (silicon wafer) using the *spin-coating* method (SpinNXG-P1H unit) and annealed for 1 h at 100 °C. The mode of application created a fixed thickness of 150±5% nm. Electrical contacts to the thin films, located at the vertices of the square silicon wafer, consisted of tungsten carbide with a diameter of 0.5 mm. The distance between contacts was 1 mm.

The phase composition of nanopowders was determined using an X-ray diffractometer Thermo ARL X'TRA (X-ray radiation, λ = 0.154 nm), which included a computer equipped with software for automatic shooting and processing of diffractograms. The initial shooting angle is 2θ = 10°, the final angle is 2θ = 70°, step = 0.02. The decoding of the obtained diffractograms was carried out using the JCPDC PCPDFWIN database [22]. In this work, the elemental composition of the obtained powders was studied by local X-ray spectral microanalysis [23] on a JEOL-6510LV installation with a Bruke energy dispersive microanalysis system. The specific surface resistance of the obtained thin films was studied by the Van der Pau method at the CIUS-4 installation. The specific surface resistance of the samples, necessary to establish gas-sensitive properties, was measured in air, as well as in the presence of the test gas (CO) with a concentration of 50 ppm. The technique was similar to that described in [24]. The required concentration of carbon monoxide was achieved by diluting the certified gas mixture with dry synthetic air. The measurements were carried out in a stationary system (a closed chamber with a volume of 50 liters). The electrical contacts to the thin films, located at the vertices of the square, consisted of tungsten carbide with a diameter of 0.5 mm. The distances between the contacts were 1 mm. Heating was carried out at a rate of 1° C/min. During the experiment, temperature control was carried out continuously. A chromel-kopel thermocouple was used for this purpose. The value of the sensor signal was determined as the ratio of the specific surface resistance in air to the specific surface resistance of samples in the presence of carbon monoxide: [25]

$$S_G = R_G / R_A,$$

where S_G – sensory signal, R_A – specific surface resistance of films in air, R_G – specific surface resistance of films in the presence of a reducing gas.

3. Results and discussion

3.1. X-ray phase analysis (XPA)

For the conformation of the expected composition, the phase composition of the nanopowders was determined using X-ray phase analysis (XPA). The obtained diffraction patterns are shown in Figs. 1 and 2. According to the results of X-ray diffractometry, the sample $LaCrO_3$ synthesized by the sol-gel method, consisted of one phase, orthorhombic lanthanum chromite. The sample $YCrO_3$ obtained by the citrate method, had one phase of yttrium chromite. Impurity phases were not detected.

According to X-ray diffraction data, $La_{0.95}Sr_{0.05}CrO_3$, $La_{0.9}Sr_{0.1}CrO_3$, $Y_{0.95}Sr_{0.05}CrO_3$, and $Y_{0.9}Sr_{0.1}CrO_3$ samples were characterized by the presence of a single phase, $YCrO_3$ and $LaCrO_3$ respectively. A shift of the peaks compared to the initial phases and a decrease in the interplanar distances of the unit cell were observed, which indicates the successful incorporation of strontium ions into the crystal lattices of yttrium chromite and lanthanum chromite. The increase in shifts and decrease in interplanar distances of unit cells for doped yttrium chromite samples correlated with the percentage content of strontium ions.

The size of the obtained particles was determined from the coherent scattering region using the Debye–Scherrer formula and was 25–

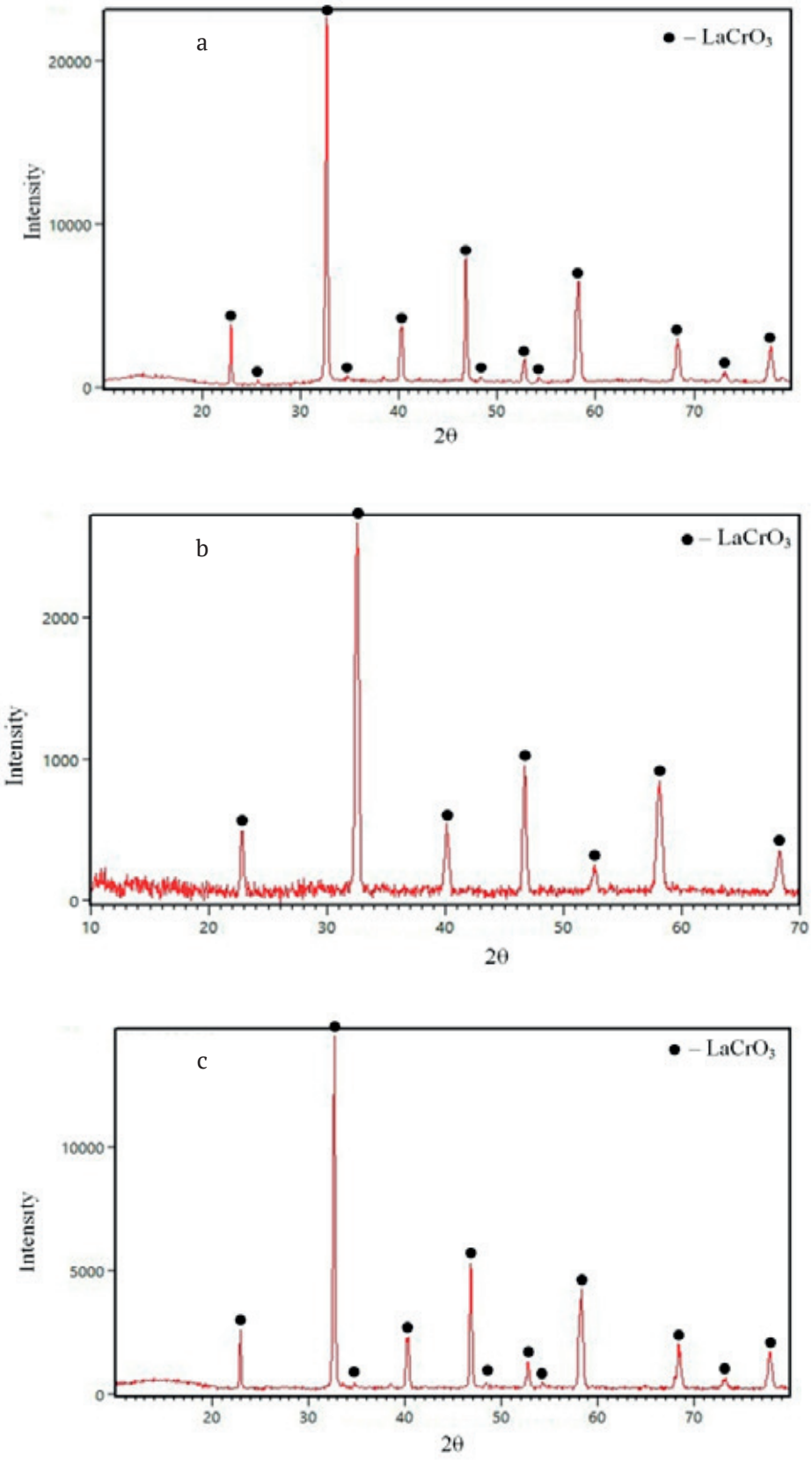

Fig. 1. X-ray diffraction patterns: a) $LaCrO_3$; b) $La_{0.95}Sr_{0.05}CrO_3$; c) $La_{0.9}Sr_{0.1}CrO_3$

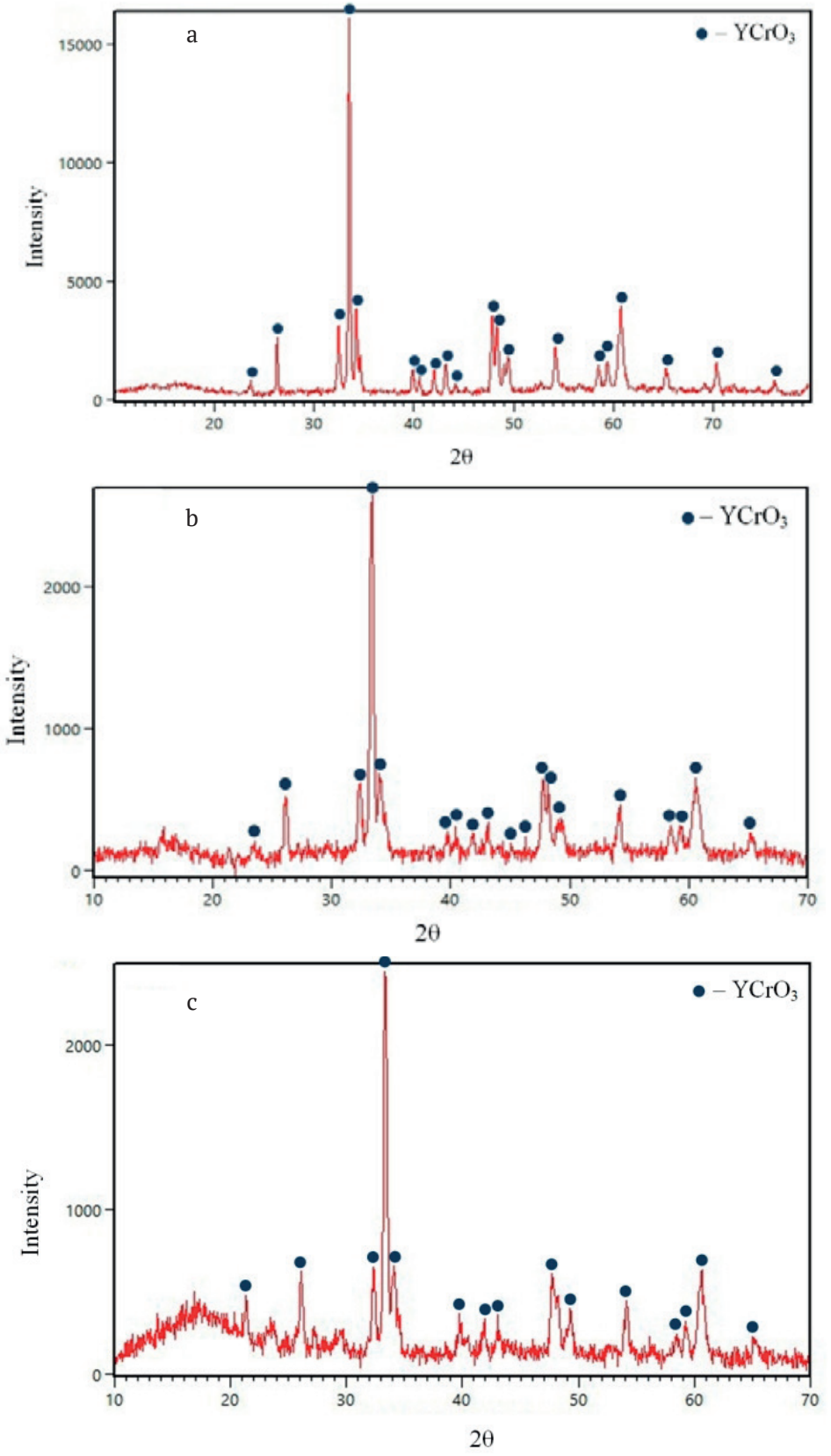

Fig. 2. X-ray diffraction patterns: a) $YCrO_3$; b) $Y_{0.95}Sr_{0.05}CrO_3$; c) $Y_{0.9}Sr_{0.1}CrO_3$

27 nm for yttrium-substituted chromites and 11–22 nm for lanthanum-substituted chromites.

3.2. Electron probe X-ray microanalysis (EPXMA)

The elemental composition of nanopowders was studied using the local X-ray spectral microanalysis (EPXMA) method. The results obtained are presented in Tables 1 and 2. The EPXMA data confirm the inclusion of strontium in $LaCrO_3$ and $YCrO_3$ lattice. The results showed that the actual composition of nanoparticles is close to their nominal composition. However, the lack of oxygen in all samples compared to the expected composition should be noted. This was a consequence of the formation of oxygen vacancies during the synthesis process and should have a beneficial effect on gas-sensitive properties, especially for yttrium ferrite.

3.3. Measurement of surface resistivity by the Van der Pauw method

Based on the results of measuring the specific surface resistance, it was found that yttrium chromite reacts to the presence of CO gas at a concentration of 50 ppm, which is shown in Fig. 3. As can be seen in Fig. 4 a response was also observed for lanthanum chromite samples, however, compared to yttrium chromite, the resistance curves had a smoother character.

The resistance of thin films of yttrium chromites at temperatures from 20 to 200 °C and samples of lanthanum chromite from 20 to 180 °C in the presence of carbon monoxide dropped sharply, which was sue to the interaction of adsorbed CO molecules with atmospheric oxygen adsorbed on the surface of the film. The following interactions occurred:

with the involvement of oxygen:

$$O_{2(gas)} \rightarrow O_{2(ads)}$$
$$O_{2(ads)} + e^- \rightarrow O^-_{2(ads)}$$
$$O^-_{2(ads)} + e^- \rightarrow 2O^-_{(ads),}$$

with the involvement of detectable gas (CO):

$$CO_{(gas)} \rightarrow CO_{(ads)}$$
$$CO_{(ads)} + O^- \rightarrow CO_{2(ads)} + e^-$$
$$CO_{2(ads)} \rightarrow CO_{2(gas).}$$

The released electrons are conduction electrons, and an increase in their concentration led to the observed decrease in surface resistance. This, in turn, indicated the electronic type of conductivity of the samples, probably caused by vacancies in the anion sublattice, the presence of which follows from the EPXMA data. At the same time, there is evidence in the literature about the possibility of lanthanum chromite and hole conduction [26].

The graphs of the dependence of the gas-sensitive response on temperature, which indicate the susceptibility of sensors based on $YCrO_3$ and $LaCrO_3$ to the studied gas are shown in Fig. 5. A directly proportional dependence of the sensory signal on the degree of doping was observed. The sensory signal increased with the increase in the strontium content.

Table 1. Results of elemental analysis of $LaCrO_3$, $La_{0.95}Sr_{0.05}CrO_3$, $La_{0.9}Sr_{0.1}CrO_3$ powder, synthesized by the sol-gel method

Nominal composition of nanoparticles	Elemental composition, at. %				The actual composition of the samples
	La	Sr	Cr	O	
$LaCrO_3$	19.41	0	20.28	60.31	$La_{0.96}CrO_{2.97}$
$La_{0.95}Sr_{0.05}CrO_3$	19.11	1.01	20.31	59.57	$La_{0.94}Sr_{0.05}CrO_{2.93}$
$La_{0.9}Sr_{0.1}CrO_3$	18.26	2.04	20.42	59.28	$La_{0.89}Sr_{0.1}CrO_{2.9}$

Table 2. Results of elemental analysis of $YCrO_3$, $Y_{0.95}Sr_{0.05}CrO_3$, $Y_{0.9}Sr_{0.1}CrO_3$ powder, obtained by the citrate method

Nominal composition of nanoparticles	Elemental composition, at. %				The actual composition of the samples
	Y	Sr	Cr	O	
$YCrO_3$	20.03	0	20.78	59.19	$Y_{0.96}CrO_{2.85}$
$Y_{0.95}Sr_{0.05}CrO_3$	19.84	0.98	20.74	58.44	$Y_{0.96}Sr_{0.047}CrO_{2.82}$
$Y_{0.9}Sr_{0.1}CrO_3$	19.53	1.97	20.66	57.84	$Y_{0.95}Sr_{0.095}CrO_{2.8}$

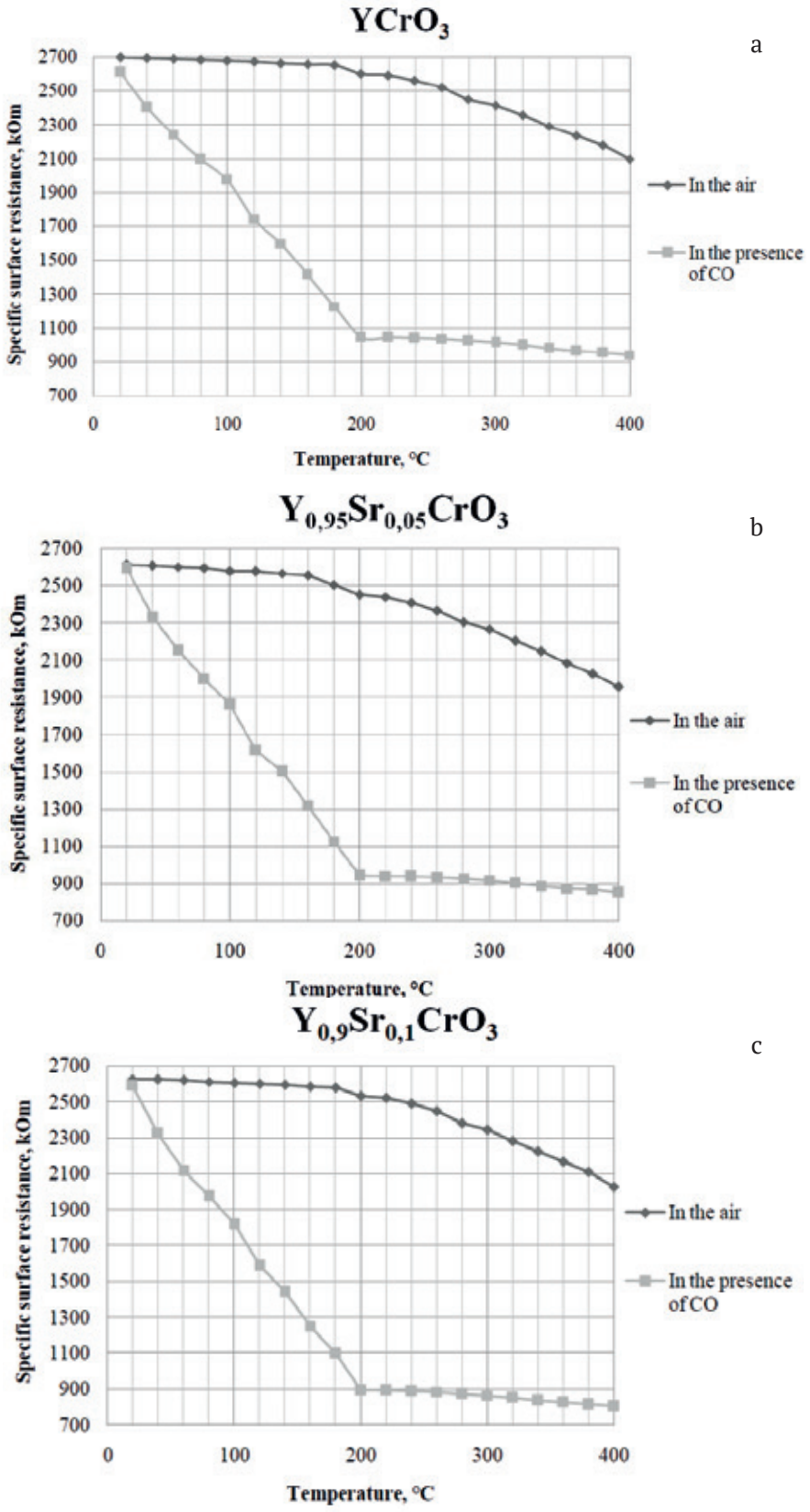

Fig. 3. Dependence of specific surface resistance on temperature in air and in the presence of CO for: a) $YCrO_3$; b) $Y_{0.95}Sr_{0.05}CrO_3$; c) $Y_{0.9}Sr_{0.1}CrO_3$

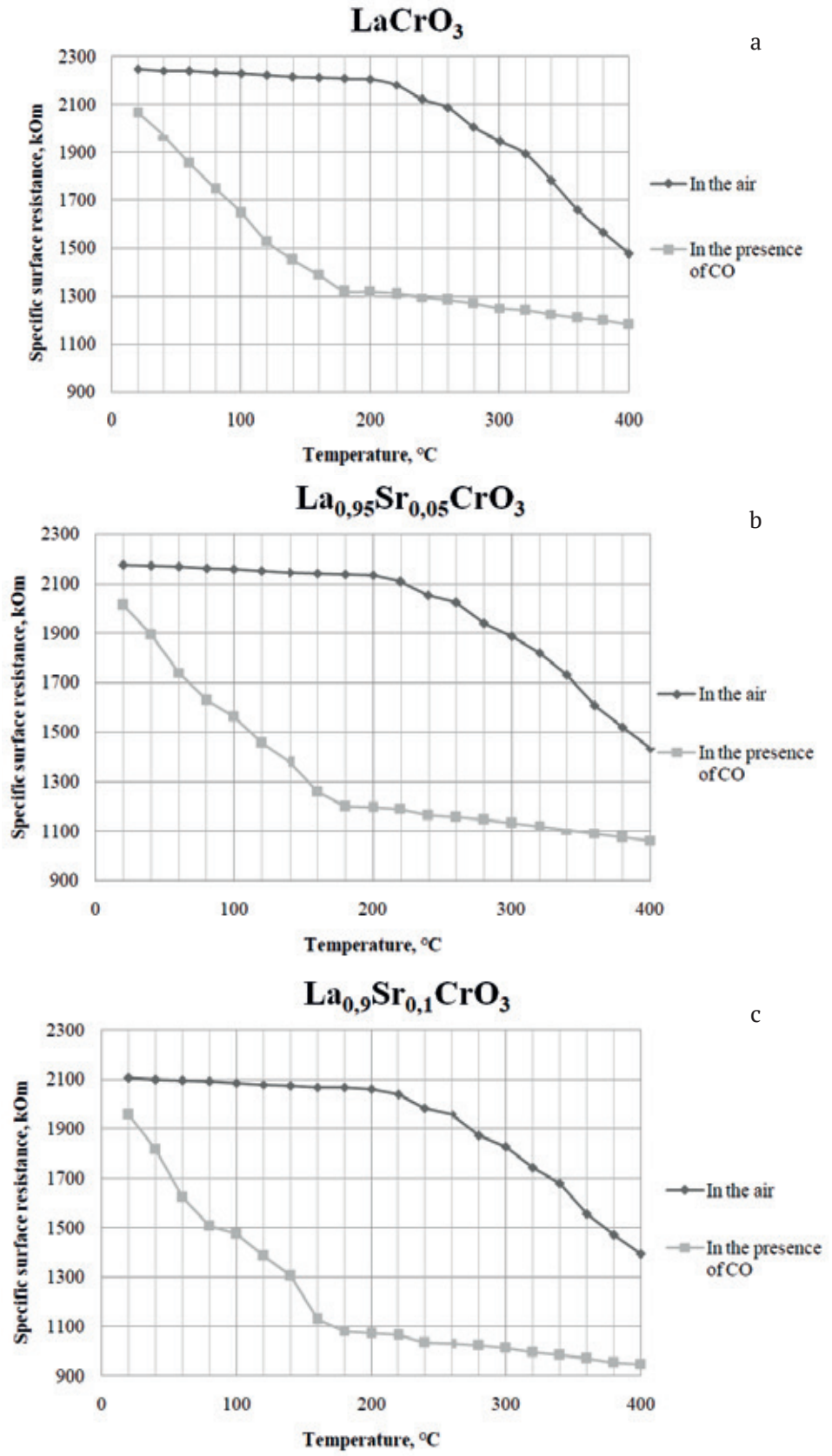

Fig. 4. Dependence of specific surface resistance on temperature in air and in the presence of CO for: a) $LaCrO_3$; b) $La_{0.95}Sr_{0.05}CrO_3$; c) $La_{0.9}Sr_{0.1}CrO_3$

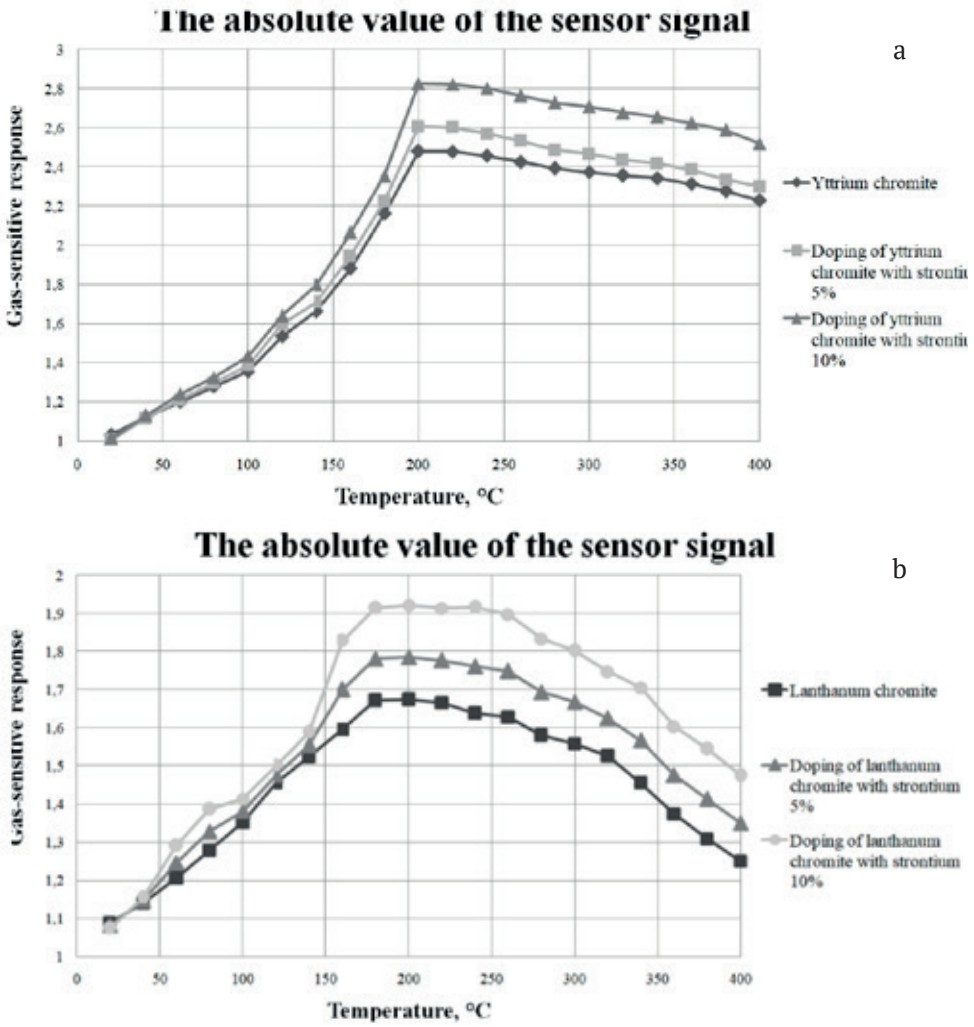

Fig. 5. Gas sensitive response as a function of temperature for: a) $YCrO_3$; b) $LaCrO_3$

At room temperature, the sensitivity of sensors in the presence of carbon monoxide was virtually absent. As the temperature increased, CO adsorption occurred on the surface of the samples. Electrons passed from adsorbed molecules into the surface layer, which reduced the specific surface resistance of nanomaterials. The maximum value of the sensor response of gas-sensitive thin films was achieved at a temperature of 200 °C for yttrium chromites. For lanthanum chromites, clearly defined maximum was not identified, and the similar value of the sensory signal was maintained in the temperature range of 180-240 °C, which was especially distinct for the sample with the maximum dopant content. The $YCrO_3$, $Y_{0.95}Sr_{0.05}CrO_3$, $Y_{0.9}Sr_{0.1}CrO_3$, $LaCrO_3$, $La_{0.95}Sr_{0.05}CrO_3$, and $La_{0.9}Sr_{0.1}CrO_3$ samples had a tendency to a linear decrease in resistance, explained by the desorption of carbon monoxide molecules with increasing temperature, and consequently, the breaking of bonds between gas molecules and surface atoms of the samples. With an increase in the strontium content, lower resistance values are detected, and the difference between the resistance in the air and in the gas under study increases.

The obtained values of the sensory signal exceed similar results known from the literature for both lanthanum chromite proper [17] and lanthanum cobaltite analogous to it [11]. It should be noted that, in comparison with the work [17], such a result was achieved simultaneously with a decrease in the concentration of the detected gas at a comparable temperature. In the case of yttrium cobaltite, the superior value of the sensor signal was achieved at a significantly higher temperature (200 °C instead of 100).

4. Conclusions

Thin films based on synthesized $YCrO_3$ and $LaCrO_3$ nanopowders were obtained using sol-gel and citrate methods and doped with 5 and 10 at. % Sr. The synthesized samples were single-phase and had a good agreement between the actual and nominal compositions. Good gas sensitivity was detected in the presence of carbon monoxide at a concentration of 50 ppm using the Van der Pauw method. The dependence of the sensory signal on the dopant content was established. The maximum sensor signal value of 2.82 corresponded to $Y_{0.9}Sr_{0.1}CrO_3$ sample at a temperature of 200 °C.

Contribution of the authors

The authors contributed equally to this article.

Conflict of interests

The authors declare that they have no known competing financial interests or personal relationships that could have influenced the work reported in this paper.

References

1. Ranga R., Kumar A., Kumari P., Singh P., Madaan V., Kumar KFerrite application as an electrochemical sensor: A review. *Materials Characterization*. 2021;178: 111269. https://doi.org/10.1016/j.matchar.2021.111269

2. Uma S., Shobana M. K. Metal oxide semiconductor gas sensors in clinical diagnosis and environmental monitoring. *Sensors and Actuators: A. Physical*. 2023;349: 114044. https://doi.org/10.1016/j.sna.2022.114044

3. Masuda Y. Recent advances in SnO_2 nanostructure based gas sensors. *Sensors and Actuators: B. Chemical*. 2022;1(2): 1–27. https://doi.org/10.1016/j.snb.2022.131876

4. Chen Y., Li H., Huang D., ... Han G. Highly sensitive and selective acetone gas sensors based on modified ZnO nanomaterials. *Materials Science in Semiconductor Processing*. 2022;43(4): 1–10. https://doi.org/10.1016/j.mssp.2022.106807

5. Petrov V. V., Bayan E. M. Investigation of rapid gas-sensitive properties degradation of ZnO-SnO_2. *Chemosensors*. 2020;8: 1–13. https://doi.org/10.3390/chemosensors8020040

6. Ryabtsev S. V., Obvintseva N. Yu., Chistyakov V. V., ... Domashevskaya E. P. Features of the resistive response to ozone of semiconductor PdO sensors operating in thermomodulation mode. *Condensed Matter and Interphases*. 2023;25(3): 392–397. https://doi.org/10.17308/kcmf.2023.25/11263

7. Rumyantseva M. N., Ivanov V. K., Shaporev A. S., ... Arbiol J. Microstructure and sensing properties of nanocrystalline indium oxide prepared using hydrothermal treatment. *Russian Journal of Inorganic Chemistry*. 2009;54(2): 163–171. https://doi.org/10.1134/s0036023609020016

8. Yadav A. K., Singhb R. K., Singha P. Fabrication of lanthanum ferrite based liquefied petroleum gas sensor. *Sensors and Actuators B: Chemical*. 2016;229: 25–30. https://doi.org/10.1016/j.snb.2016.01.066

9. Hu J., Chen X., Zhang Y. Batch fabrication of formaldehyde sensors based on $LaFeO_3$ thin film with ppb-level detection limit. *Sensors and Actuators: B. Chemical*. 2021;349: 130738. https://doi.org/10.1016/j.snb.2021.130738

10. Qina J., Cui Z., Yanga X., Zhua S., Li Z., Lianga Y. Synthesis of three-dimensionally ordered macroporous $LaFeO_3$ with enhanced methanol gas sensing properties. *Sensors and Actuators B: Chemical*. 2015;209: 706–713. https://doi.org/10.1016/j.snb.2014.12.046

11. Chumakova V. T., Marikutsa A. V., Rumyantseva M. N. Nanocrystalline lanthanum cobaltite as a material for gas sensors. *Russian Journal of Applied Chemistry*. 2021;94(12): 1651–1698. https://doi.org/10.1134/s1070427221120119

12. Tiwari S., Saleem M. Varshney M., Mishra A., Varshney D. Structural, optical and magnetic studies of $YCrO_3$ perovskites. *Physica B: Condensed Matter*. 2018;546: 67–72. https://doi.org/10.1063/1.5122339

13. Kadu A. V., Bodade A. B., Bodade A. B., Chaudhari G. N. Structural characterization of nanocrystalline $La_{1-x}Sr_xCrO_3$ thick films for H_2S gas sensors. *Journal of Sensor Technology*. 2012;2: 13–18. https://doi.org/10.4236/jst.2012.21003

14. Khetre S. M., Chopade A. U., Khilare C. J., Jadhav H. V., Jagadale P. N., Bamane S. R. Electrical and dielectric properties of nanocrystalline $LaCrO_3$. *Journal of Materials Science: Materials in Electronics*. 2013;24: 4361–4366. https://doi.org/10.1007/s10854-013-1411-z

15. Matulkova I., Holec P., Pacakova B., ... Vejpravova J. On preparation of nanocrystalline chromites by co-precipitation and autocombustion methods. *Sensors and Actuators A: Physical*. 2015;195: 66–73. https://doi.org/10.1016/j.mseb.2015.01.011

16. Rao V., Rajamani M., Ranjith R., David A., Prellier W. Local structural distortion and interrelated phonon mode studies in yttrium chromite. *Materials Research Society*. 2017;32(8): 1541–1547. https://doi.org/10.1557/jmr.2017.5

17. Prashant B. K., Kailas H. K., Uday G. D., Umesh J. T., Sachin G. S. Fabrication of thin film sensors by spin coating using sol-gel $LaCrO_3$ perovskite material modified with transition metals for sensing

environmental pollutants, greenhouse gases and relative humidity. *Environmental Challenges*. 2021;3: 1–13. https://doi.org/10.1016/j.envc.2021.100043

18. Chadli I., Omari M., Abu Dalo M., Albiss B. Preparation by sol–gel method and characterization of Zn-doped $LaCrO_3$ perovskite. *Journal of Sol-Gel Sci Technol*. 2016;80: 598–605. https://doi.org/10.1007/s10971-016-4170-5

19. Zarrin N., Husain S., Khan W., Manzoor S. Sol-gel derived cobalt doped $LaCrO_3$: Structure and physical properties. *Journal of Alloys and Compounds*. 2019;784(5): 541–555. https://doi.org/10.1016/j.jallcom.2019.01.018

20. Nguyen A. T., Tran H. L. T., Nguyen Ph. U. T.,... Nguyen T. L. Sol-gel synthesis and the investigation of the properties of nanocrystalline holmium orthoferrite. *Nanosystems: Physics, Chemistry, Mathematics*. 2020;11(6): 698–704. https://doi.org/10.17586/2220-8054-2020-11-6-698-704

21. Mittova I. Ya., Perov N. S., Alekhina Iu. A., ... Sladkopevtsev B. V. Size and magnetic characteristics of $YFeO_3$ nanocrystals. *Inorganic Materials*. 2022;58(3): 271–277. https://doi.org/10.1134/S0020168522030116

22. JCPDC PCPDFWIN: A Windows Retrieval. Display program for Accessing the ICDD PDF. 2 Data base, Inernation Centre for Diffraction Data. 1997.

23. Krishtal M. M., Jasnikov I. S., Polunin V. I., Filatov A. M., Ul'janenkov A.G. *Scanning electron microscopy and X-ray microanalysis*[*]. Moscow: Tehnosfera Publ.; 2009. 208 p.

24. Kostryukov V. F., Parshina A. S., Sladkopevtsev B. V., Mittova I. Ya. Thin films on the surface of GaAs, obtained by chemically stimulated thermal oxidation, as materials for gas sensors. *Coatings (MDPI)*. 2022;12(12): 1819–1828. https://doi.org/10.3390/coatings12121819

25. Kostryukov V. F., Balasheva D. S., Parshina A. S. Creation of thin films on the surface of InP with a controlled gas-sensitive signal under the influence of $PbO + Y_2O_3$ compositions. *Condensed Matter and Interphases*. 2021;23(3): 406–412. https://doi.org/10.17308/kcmf.2021.23/3532

26. Shevchik A.P. Suvorov S.A. Jelektroprovodjashhie svojstva materialov na osnove hromita lantana. Izvestija sankt-peterburgskogo gosudarstvennogo tehnologicheskogo instituta (tehnicheskogo universiteta). 2008;3(29): 36–41.

Information about the authors

Milena A. Yakimchuk, Master's student of the Department of Materials Science and Industry of Nanosystems, Voronezh State University (Voronezh, Russian Federation).

yakimchuk.720.46@gmail.com

Eugenia S. Eliseeva, student of the Department of Materials Science and Industry of Nanosystems, Voronezh State University (Voronezh, Russian Federation).

eliseewa.zhenya@yandex.ru

Victor F. Kostryukov, Dr. Sci. (Chem.), Associate Professor, Associate Professor of the Department of Materials Science and Industry of Nanosystems, Voronezh State University (Voronezh, Russian Federation).

https://orcid.org/0000-0001-5753-5653

vc@chem.vsu.ru

Received 23.04.2024; approved after reviewing 02.08.2024; accepted for publication 15.08.2024; published online 01.10.2024.

Translated by Valentina Mittova